


Search for $D^0 \rightarrow K^- \eta e^+ \nu_e$, $D^+ \rightarrow K_S^0 \eta e^+ \nu_e$ and $D^+ \rightarrow \eta \eta e^+ \nu_e$ decays

M. Ablikim *et al.**
(BESIII Collaboration)

 (Received 24 September 2024; accepted 11 November 2024; published 2 December 2024)

By analyzing e^+e^- annihilation data corresponding to an integrated luminosity of 7.93 fb^{-1} , collected at the center-of-mass energy of 3.773 GeV with the BESIII detector, we search for the semileptonic decays $D^0 \rightarrow K^- \eta e^+ \nu_e$, $D^+ \rightarrow K_S^0 \eta e^+ \nu_e$ and $D^+ \rightarrow \eta \eta e^+ \nu_e$ for the first time. We present evidence for $D^0 \rightarrow K^- \eta e^+ \nu_e$ with a significance of 3.3σ . The branching fraction of $D^0 \rightarrow K^- \eta e^+ \nu_e$ is measured to be $(0.84_{-0.34}^{+0.29} \pm 0.22) \times 10^{-4}$. No significant signals are observed for the decays $D^+ \rightarrow K_S^0 \eta e^+ \nu_e$ and $D^+ \rightarrow \eta \eta e^+ \nu_e$ and we set the upper limits on their branching fractions.

DOI: [10.1103/PhysRevD.110.112001](https://doi.org/10.1103/PhysRevD.110.112001)

I. INTRODUCTION

Studies of the semileptonic D decays are important to test the Standard Model (SM) and search for new physics beyond the SM [1]. Four-body semileptonic decays $D \rightarrow P_1 P_2 \ell^+ \nu_\ell$ (P denotes the pseudoscalar meson), mediated via $c \rightarrow (s, d) \ell^+ \nu_\ell$ transitions, can receive contributions from light scalar or vector meson. Consequently, these decays provide a good laboratory for probing the internal structures of light hadrons [2–4]. The experimental studies of the semileptonic decays $D \rightarrow P_1 P_2 \ell^+ \nu_\ell$, except for the decays $D \rightarrow (V, S) \ell^+ \nu_\ell$ with $(V, S) \rightarrow P_1 P_2$ (V, S denote a vector or scalar meson), are limited. The semileptonic decays $D^0 \rightarrow K^- \eta e^+ \nu_e$, $D^+ \rightarrow K_S^0 \eta e^+ \nu_e$ and $D^+ \rightarrow \eta \eta e^+ \nu_e$ proceed via the Feynman diagrams shown in Fig. 1.

Throughout this paper, D denotes a D^0 or D^+ meson. The branching fractions of $D^0 \rightarrow K^- \eta e^+ \nu_e$, $D^+ \rightarrow K_S^0 \eta e^+ \nu_e$ and $D^+ \rightarrow \eta \eta e^+ \nu_e$ decays are predicted [5] using SU(3) flavor symmetry theory, as summarized in Table I. The branching fractions of $D \rightarrow V/S e^+ \nu_e$ (where V and S denote $K_0^*(1430)$ and $f_0(1500)$, respectively) are predicted using the covariant light-front quark model [6]. No experimental study of these decays has been reported to date.

In this paper, we search for the semileptonic decays $D^0 \rightarrow K^- \eta e^+ \nu_e$, $D^+ \rightarrow K_S^0 \eta e^+ \nu_e$ and $D^+ \rightarrow \eta \eta e^+ \nu_e$ for the first time, using an integrated luminosity of 7.93 fb^{-1} of e^+e^- collision data taken with the BESIII detector at the center-of-mass energy of $\sqrt{s} = 3.773 \text{ GeV}$. Charge-conjugate modes are implied throughout this paper.

*Full author list given at the end of the article.

Published by the American Physical Society under the terms of the [Creative Commons Attribution 4.0 International license](https://creativecommons.org/licenses/by/4.0/). Further distribution of this work must maintain attribution to the author(s) and the published article's title, journal citation, and DOI. Funded by SCOAP³.

II. BESIII DETECTOR AND MONTE CARLO SIMULATION

The BESIII detector [7] records symmetric e^+e^- collisions provided by the BEPCII storage ring [8] in the center-of-mass energy range from 1.85 to 4.95 GeV , with a peak luminosity of $1 \times 10^{33} \text{ cm}^{-2} \text{ s}^{-1}$ achieved at $\sqrt{s} = 3.773 \text{ GeV}$. BESIII has collected large data samples in this energy region. The cylindrical core of the BESIII detector covers 93% of the full solid angle and consists of a helium-based multilayer drift chamber (MDC), a plastic scintillator time-of-flight system (TOF), and a CsI(Tl) electromagnetic calorimeter (EMC), which are all enclosed in a superconducting solenoidal magnet providing a 1.0 T magnetic field. The solenoid is supported by an octagonal flux-return yoke with resistive plate counter muon identification modules interleaved with steel. The charged-particle momentum resolution at $1 \text{ GeV}/c$ is 0.5% , and the dE/dx resolution is 6% for electrons from Bhabha scattering. The EMC measures photon energies with a resolution of 2.5% (5%) at 1 GeV in the barrel (end cap) region. The time resolution in the TOF barrel region is 68 ps , while that in the end cap region was 110 ps . The end cap TOF system was upgraded in 2015 using multigap resistive plate chamber technology, providing a time

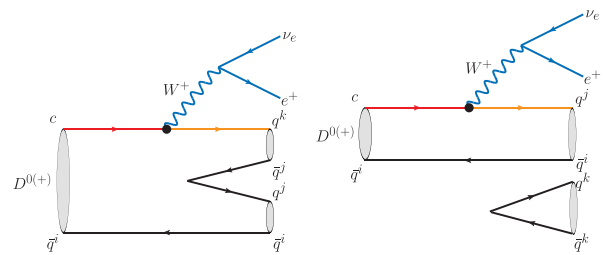


FIG. 1. Two possible leading-order Feynman diagrams of the nonresonant decays $D^0 \rightarrow K^- \eta e^+ \nu_e$, $D^+ \rightarrow K_S^0 \eta e^+ \nu_e$ and $D^+ \rightarrow \eta \eta e^+ \nu_e$.

TABLE I. The branching fractions of $D^0 \rightarrow K^- \eta e^+ \nu_e$, $D^+ \rightarrow \bar{K}^0 \eta e^+ \nu_e$ and $D^+ \rightarrow \eta \eta e^+ \nu_e$ predicted using SU(3) flavor symmetry [5].

Decay	$D^0 \rightarrow K^- \eta e^+ \nu_e$	$D^+ \rightarrow \bar{K}^0 \eta e^+ \nu_e$	$D^+ \rightarrow \eta \eta e^+ \nu_e$
Value ($\times 10^{-6}$)	3.51 ± 3.51	8.9 ± 8.9	3.16 ± 2.26

resolution of 60 ps. About 63% of the data used in this analysis benefits from this upgrade.

Simulated data samples produced with a GEANT4-based [9] Monte Carlo (MC) package, which includes the geometric description of the BESIII detector and the detector response, are used to determine detection efficiencies and to estimate backgrounds. The simulation models the beam energy spread and initial state radiation (ISR) in the e^+e^- annihilations with the generator KKMC [10,11]. The inclusive MC samples include the production of $D\bar{D}$ pairs (including quantum coherence for the neutral D channels), the non- $D\bar{D}$ decays of the $\psi(3770)$, the ISR production of J/ψ and $\psi(3686)$ states, and the continuum processes incorporated in KKMC [10,11]. All particle decays are modeled with EVTGEN [12,13] using the branching fractions either taken from the Particle Data Group [14] when available, or otherwise estimated with LUNDCHARM [15]. Final state radiation (FSR) from charged final state particles is incorporated using the PHOTOS package [16]. Because there is little information about the decays under study, the signal decays $D \rightarrow P \eta e^+ \nu_e$ are simulated, proceeding with and without subresonance, with a fraction of half for each. For the first case, they are generated as $D \rightarrow \mathcal{R} e^+ \nu_e$ with $\mathcal{R} \rightarrow P \eta$ by using the ISGW2 model [17], where $P = K, K_S^0$, and η . For the second case, called phase-space (PHSP) model, they are generated in N-body decays, averaging over the spins of initial and final state particles.

III. MEASUREMENT METHOD

The $e^+e^- \rightarrow \psi(3770) \rightarrow D\bar{D}$ process provides an ideal platform to investigate semileptonic D decays by using the double-tag (DT) method [18,19], benefiting from the fact that there is no additional particle accompanying the $D\bar{D}$ pair in the final state. First, single-tag (ST) \bar{D}^0 mesons are reconstructed by using the hadronic decay modes $\bar{D}^0 \rightarrow K^+ \pi^-$, $K^+ \pi^- \pi^0$, and $K^+ \pi^- \pi^- \pi^+$, while ST D^- mesons are reconstructed via the decays $D^- \rightarrow K^+ \pi^- \pi^-$, $K_S^0 \pi^-$, $K^+ \pi^- \pi^- \pi^0$, $K_S^0 \pi^- \pi^0$, $K_S^0 \pi^+ \pi^- \pi^-$, and $K^+ K^- \pi^-$. Then, signal candidates are reconstructed from the remaining tracks and showers. Candidates in which $D^0 \rightarrow K^- \eta e^+ \nu_e$, $D^+ \rightarrow K_S^0 \eta e^+ \nu_e$ or $D^+ \rightarrow \eta \eta e^+ \nu_e$ with \bar{D} decays into an ST mode are called DT candidates. The branching fractions of the signal decays are determined by

$$\mathcal{B}_{\text{SL}} = \frac{N_{\text{DT}}}{N_{\text{ST}}^{\text{tot}} \cdot \bar{\epsilon}_{\text{SL}} \cdot \mathcal{B}_{\text{sub}}}, \quad (1)$$

where $N_{\text{ST}}^{\text{tot}}$ represents the total number of ST \bar{D} mesons, N_{DT} denotes the number of the DT events, \mathcal{B}_{sub} is $\mathcal{B}_{\eta \rightarrow \gamma \gamma}$, $\mathcal{B}_{K_S^0 \rightarrow \pi^+ \pi^-} \cdot \mathcal{B}_{\eta \rightarrow \gamma \gamma}$, and $\mathcal{B}_{\eta \rightarrow \gamma \gamma}^2$ for the decays $D^0 \rightarrow K^- \eta e^+ \nu_e$, $D^+ \rightarrow K_S^0 \eta e^+ \nu_e$ and $D^+ \rightarrow \eta \eta e^+ \nu_e$, respectively. $\mathcal{B}_{K_S^0 \rightarrow \pi^+ \pi^-}$ and $\mathcal{B}_{\eta \rightarrow \gamma \gamma}$ are the branching fractions of $K_S^0 \rightarrow \pi^+ \pi^-$ and $\eta \rightarrow \gamma \gamma$. Additionally, $\bar{\epsilon}_{\text{SL}}$ is the average efficiency of reconstructing the semileptonic signal decays. The average signal efficiency, weighted over the ST modes i , is calculated as $\bar{\epsilon}_{\text{SL}} = \sum_i [(\epsilon_{\text{DT}}^i \cdot N_{\text{ST}}^i) / (\epsilon_{\text{ST}}^i \cdot N_{\text{ST}}^{\text{tot}})]$, where N_{ST}^i is the ST yield of $\bar{D} \rightarrow i$, ϵ_{ST}^i is the detection efficiency of reconstructing $\bar{D} \rightarrow i$, and ϵ_{DT}^i is the detection efficiency of reconstructing the ST \bar{D} and the signal decay simultaneously.

IV. SELECTION OF ST \bar{D} CANDIDATES

All charged tracks used in this analysis are required to be within a polar angle (θ) range of $|\cos \theta| < 0.93$, where θ is defined with respect to the z -axis, which is the symmetry axis of the MDC. For good charged tracks not originating from K_S^0 decays, the distance of closest approach to the interaction point (IP) must be less than 10 cm along the z -axis, $|V_z|$, and less than 1 cm in the transverse plane, $|V_{xy}|$. Charged tracks are identified by using the energy deposited in the MDC (dE/dx) and the flight time in the TOF; combined likelihoods for the pion and kaon hypotheses (\mathcal{L}_K and \mathcal{L}_π) are computed separately. Kaon and pion candidates are required to satisfy $\mathcal{L}_K > \mathcal{L}_\pi$ and $\mathcal{L}_\pi > \mathcal{L}_K$, respectively.

Each K_S^0 candidate meson is reconstructed from two oppositely charged tracks each satisfying $|V_z| < 20$ cm. The two charged tracks are assigned as $\pi^+ \pi^-$ without imposing further particle identification (PID) criteria. They are constrained to originate from a common vertex, which is required to be away from the IP by a flight distance of at least twice the vertex resolution. The quality of the vertex fits (a primary vertex fit and a secondary vertex fit for K_S^0) is ensured by a requirement of $\chi^2 < 100$, where the number of degrees of freedom is 3. The invariant mass of the $\pi^+ \pi^-$ pair is required to be within (0.487, 0.511) GeV/ c^2 .

Neutral pion candidates are reconstructed by the $\pi^0 \rightarrow \gamma \gamma$ decays. Photon candidates are identified using showers in the EMC. The deposited energy of each shower must be more than 25 MeV in the barrel region ($|\cos \theta| < 0.80$) and more than 50 MeV in the end cap region ($0.86 < |\cos \theta| < 0.92$) [7]. To exclude showers that originate from charged tracks, the angle subtended at the IP by the EMC shower and the position of the closest charged track at the EMC must be greater than 10 degrees. To suppress electronic noise and showers unrelated to the event, the difference between the EMC shower time and the event start time is required to be within [0, 700] ns. For π^0 candidates, the invariant mass of the photon pair is required to be within (0.115, 0.150) GeV/ c^2 . To improve the momentum resolution, a mass-constrained (1-C) fit to

TABLE II. The ΔE requirements, the obtained ST $\bar{D}^0(D^-)$ yields (N_{ST}^i) in data and the ST efficiencies (ϵ_{ST}^i). The efficiencies do not include the branching fractions of the K_S^0 and π^0 decays. The uncertainties are statistical only.

Tag mode	ΔE (GeV)	$N_{\text{ST}}^i (\times 10^3)$	$\epsilon_{\text{ST}}^i (\%)$
$\bar{D}^0 \rightarrow K^+ \pi^-$	(-0.027, 0.027)	1449.5 \pm 1.3	64.95 \pm 0.01
$\bar{D}^0 \rightarrow K^+ \pi^- \pi^0$	(-0.062, 0.049)	2913.2 \pm 2.0	35.52 \pm 0.01
$\bar{D}^0 \rightarrow K^+ \pi^+ \pi^- \pi^-$	(-0.026, 0.024)	1944.2 \pm 1.6	40.42 \pm 0.01
$D^- \rightarrow K^+ \pi^- \pi^-$	(-0.025, 0.024)	2164.0 \pm 1.6	51.17 \pm 0.01
$D^- \rightarrow K_S^0 \pi^-$	(-0.025, 0.026)	250.4 \pm 0.5	50.63 \pm 0.02
$D^- \rightarrow K^+ \pi^- \pi^- \pi^0$	(-0.057, 0.046)	689.0 \pm 1.2	25.50 \pm 0.01
$D^- \rightarrow K_S^0 \pi^- \pi^0$	(-0.062, 0.049)	558.5 \pm 0.9	26.28 \pm 0.01
$D^- \rightarrow K_S^0 \pi^- \pi^- \pi^+$	(-0.028, 0.027)	300.5 \pm 0.7	28.97 \pm 0.01
$D^- \rightarrow K^+ K^- \pi^-$	(-0.024, 0.023)	187.4 \pm 0.5	41.06 \pm 0.02

the nominal π^0 mass [14]; a fit $\chi^2 < 50$ is also required, where the number of degrees of freedom is 1.

In the selection of $\bar{D}^0 \rightarrow K^+ \pi^-$ candidates, the backgrounds from cosmic rays and Bhabha events are rejected by using the same requirements described in Ref. [20]. To separate the ST \bar{D} mesons from combinatorial backgrounds, we define the energy difference $\Delta E \equiv E_{\bar{D}} - E_{\text{beam}}$ and the beam-constrained mass $M_{\text{BC}} \equiv \sqrt{E_{\text{beam}}^2/c^4 - |\vec{p}_{\bar{D}}|^2/c^2}$, where E_{beam} is the beam energy, and $E_{\bar{D}}$ and $\vec{p}_{\bar{D}}$ are the total energy and momentum of the ST \bar{D} candidate in the e^+e^- center-of-mass frame. If there is more than one \bar{D}

candidate in a specific ST mode, the one with the minimum $|\Delta E|$ value is kept for further analysis. The corresponding $|\Delta E|$ requirements for each ST modes are listed in Table II. To extract the yield of ST \bar{D} mesons for each mode, a fit is performed to the corresponding M_{BC} distribution. The signal is described by an MC-simulated shape convolved with a double-Gaussian function which compensates the resolution difference between data and MC simulation. The background is described by an ARGUS function [21]. All fit parameters are left free in the fits. Figure 2 shows the fits to the M_{BC} distributions for individual ST modes. Candidates within the M_{BC} signal region of (1.864, 1.876) GeV/c^2 , shown as red arrows in Fig. 2, are kept for further analysis. Combining the contributions from all ST modes, the total yields of ST \bar{D}^0 and D^- mesons are obtained to be $N_{\text{ST}, \bar{D}^0}^{\text{tot}} = (6306.9 \pm 2.8_{\text{stat}}) \times 10^3$ and $N_{\text{ST}, D^-}^{\text{tot}} = (4149.9 \pm 2.4_{\text{stat}}) \times 10^3$, respectively.

V. SELECTION OF DT $\bar{D}\bar{D}$ EVENTS

In the presence of the ST \bar{D} candidates, signal decays are reconstructed from charged tracks and showers which have not been used in the ST selection. It is required that there are exactly two, three, or one charged tracks reconstructed in $D^0 \rightarrow K^- \eta e^+ \nu_e$, $D^+ \rightarrow K_S^0 \eta e^+ \nu_e$, or $D^+ \rightarrow \eta \eta e^+ \nu_e$ decays, respectively.

The positron candidate is required to have a charge opposite to that of the charm quark in the ST \bar{D} meson. Information from dE/dx , TOF, and the EMC measurements is combined to create combined likelihoods under the positron, pion, and kaon hypotheses (\mathcal{L}_e , \mathcal{L}_π , and \mathcal{L}_K). The positron candidate is required to satisfy $\mathcal{L}_e > 0.001$ and $\mathcal{L}_e / (\mathcal{L}_e + \mathcal{L}_\pi + \mathcal{L}_K) > 0.8$. To reduce background from hadrons and muons, the positron candidate is further required to have an E/p , the deposited energy in the EMC divided by the momentum measured in the MDC, between 0.8 and 1.1.

The invariant mass of the η candidate photon pair is required to be within (0.505, 0.575) GeV/c^2 . To improve the momentum resolution, a mass-constrained (1-C) fit to the nominal η mass [14] is imposed on the photon pair. The fit χ^2 must be less than 50 and the four-momentum of the η candidate returned by this kinematic fit is used for further analysis. The selection criteria of photons, charged and neutral kaons are the same as those used in the ST selection.

Peaking backgrounds from hadronic D decays with multiple pions in the final states are rejected by requiring that the invariant mass of the $P\eta e^+$ system, $M_{P\eta e^+}$, be less than 1.80 GeV/c^2 . To suppress backgrounds with extra photon(s), we require that the energy of any extra photon, $E_{\text{extra}}^{\gamma}$, be less than 0.25 GeV and there is no extra π^0 ($N_{\text{extra}}^{\pi^0} = 0$) in the candidate event. To reject the background from non- η decays, such as $D^0 \rightarrow K^- \pi^0 e^+ \nu_e$, $K^- \pi^+ \pi^0 \pi^0$, in the $D^0 \rightarrow K^- \eta e^+ \nu_e$ analysis, we require the invariant mass of the $K^- \eta$ system to satisfy $M_{K^- \eta} > 1.30 \text{ GeV}/c^2$.

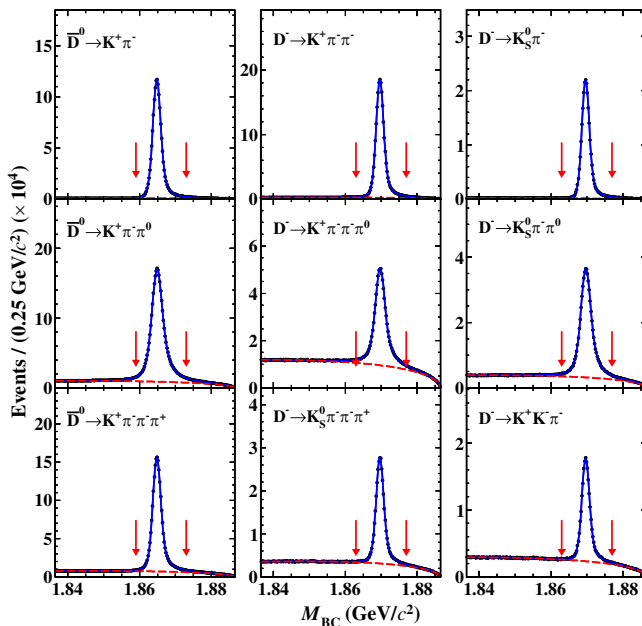


FIG. 2. The M_{BC} distributions for the different ST \bar{D} decays with fit results overlaid. In each plot, the points with error bars are data, the red dashed curve is the background contribution, and the blue solid line shows the total fit. Pairs of red arrows show the M_{BC} signal windows.

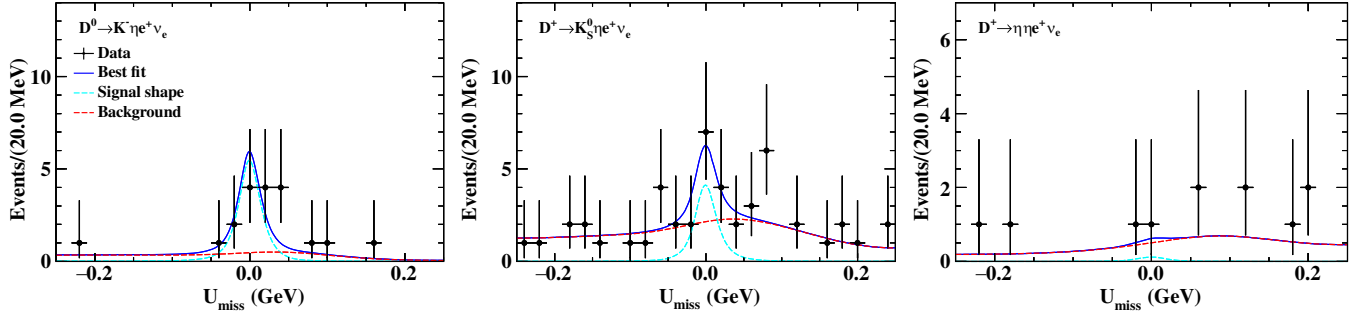


FIG. 3. The U_{miss} distributions of the $D^0 \rightarrow K^-\eta e^+\nu_e$, $D^+ \rightarrow K_S^0\eta e^+\nu_e$ and $D^+ \rightarrow \eta\eta e^+\nu_e$ candidate events with fit results overlaid. The points with error bars are data, the light blue dashed curve is the signal, the red dashed curve is the background contribution, and the blue solid curve shows the total fit.

The neutrino cannot be directly detected in the BESIII detector. Instead, information about the missing neutrino is inferred by the kinematic quantity $U_{\text{miss}} \equiv E_{\text{miss}} - |\vec{p}_{\text{miss}}|$. Here, E_{miss} and \vec{p}_{miss} are the missing energy and momentum of the semileptonic candidate, respectively, calculated by $E_{\text{miss}} \equiv E_{\text{beam}} - \sum_j E_j$ and $\vec{p}_{\text{miss}} \equiv \vec{p}_D - \sum_j \vec{p}_j$ in the e^+e^- center-of-mass frame. The index j sums over the P , η and e^+ in the signal candidate, and E_j and \vec{p}_j are the energy and momentum of the j th particle, respectively. To improve the U_{miss} resolution, the D energy is constrained to the beam energy and $\vec{p}_D \equiv -\hat{p}_{\bar{D}} \sqrt{E_{\text{beam}}^2 - m_D^2}$, where $\hat{p}_{\bar{D}}$ is the unit vector in the direction of the ST \bar{D} momentum, and m_D is the D nominal mass [14]. For correctly reconstructed signal events, U_{miss} peaks at zero.

The detection efficiencies $\bar{\epsilon}_{\text{SL}}$ for $D^0 \rightarrow K^-\eta e^+\nu_e$, $D^+ \rightarrow K_S^0\eta e^+\nu_e$ and $D^+ \rightarrow \eta\eta e^+\nu_e$ are $(5.29 \pm 0.05)\%$, $(7.79 \pm 0.05)\%$, and $(7.52 \pm 0.05)\%$, respectively.

Figure 3 shows the U_{miss} distributions of the accepted candidate events. To extract the signal yields of each signal decay, we perform an unbinned maximum likelihood fit on the corresponding U_{miss} distribution. In the fit, the signal and background components are characterized by the simulated shapes obtained from the signal MC events

and the inclusive MC sample, respectively, with signal and background yields floating.

Evidence for the decay $D^0 \rightarrow K^-\eta e^+\nu_e$ is found with a statistical significance of 3.3σ . The branching fraction of the decay $D^0 \rightarrow K^-\eta e^+\nu_e$ is determined to be $(0.68_{-0.23}^{+0.27}) \times 10^{-4}$. As no significant signals are observed for the $D^+ \rightarrow K_S^0\eta e^+\nu_e$ and $D^+ \rightarrow \eta\eta e^+\nu_e$ decays, the upper limits on their branching fractions are set at the 90% confidence level (CL). The blue dotted curves in Fig. 4 show the normalized likelihood distributions versus the corresponding products of branching fractions.

VI. SYSTEMATIC UNCERTAINTY

With the DT method, many systematic uncertainties associated with the ST selection cancel out in the branching fraction measurements. The sources of the systematic uncertainties in the measurements of the product of branching fractions are categorized into multiplicative and additive systematic uncertainties for the decays $D^+ \rightarrow K_S^0\eta e^+\nu_e$ and $D^+ \rightarrow \eta\eta e^+\nu_e$. However, the sources of the systematic uncertainties are not classified for the $D^0 \rightarrow K^-\eta e^+\nu_e$ decay. Multiplicative systematic uncertainties

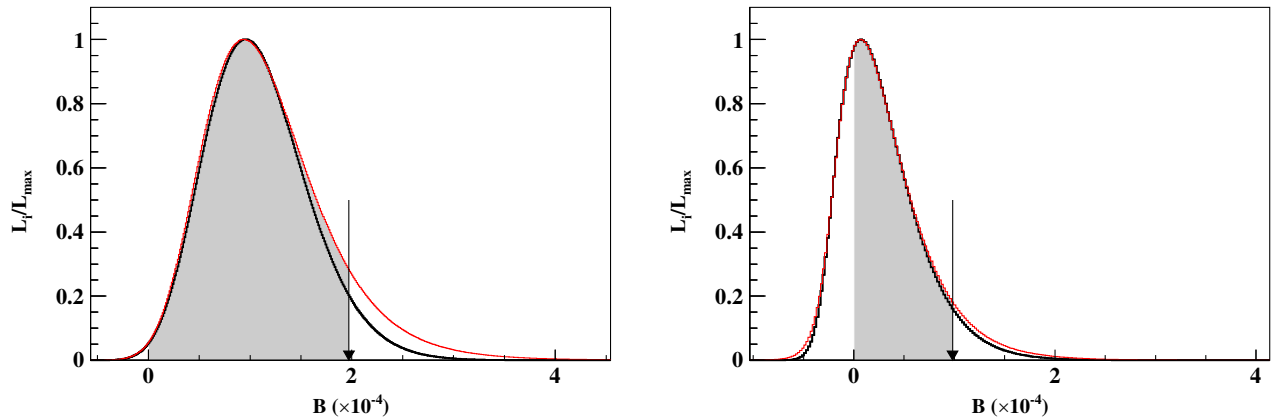


FIG. 4. The normalized likelihood distributions versus the product of branching fractions of $D^+ \rightarrow K_S^0\eta e^+\nu_e$ (left) and $D^+ \rightarrow \eta\eta e^+\nu_e$ (right). The red solid (black dotted) curves indicate results including (not including) systematic uncertainties. The black arrows show the upper limits on the branching fractions at the 90% confidence level.

include sources of uncertainty related to various efficiencies and are assigned relative to the measured branching fractions. The uncertainty associated with the ST yield $N_{\text{ST}}^{\text{tot}}$ is estimated to be 0.1% due to the fit to the M_{BC} distributions, which is studied by varying the signal and background shapes. The uncertainties of the quoted branching fractions of $K_S^0 \rightarrow \pi^+ \pi^-$ and $\eta \rightarrow \gamma \gamma$ are 0.07% and 0.5% [14], respectively. The uncertainties from the tracking and PID of e^\pm are studied with a control sample of $e^+ e^- \rightarrow \gamma e^+ e^-$. The uncertainties from the tracking and PID of K^\pm and π^0 reconstruction are obtained by studying a DT control sample $\psi(3770) \rightarrow D \bar{D}$ with hadronic D decays. The systematic uncertainties from the tracking (PID) efficiencies are assigned as 1.0% (1.0%) per e^\pm and 1.0% (1.0%) per K^\pm , respectively [22]. Due to the limited sample size, the systematic uncertainty of the η reconstruction is estimated by referring to that of π^0 , which includes photon efficiency, mass window selection, and invariant mass constraint imposed by kinematic fit. The systematic uncertainty of η is taken to be 1.0% per η . The systematic uncertainty associated with the K_S^0 reconstruction is assigned to be 1.7% based on control samples of $\psi(3770) \rightarrow D \bar{D}$. The systematic uncertainties from the $E_{\text{extray}}^{\text{max}}$, $N_{\text{extra}}^{\text{char}}$ and $N_{\text{extra}}^{\pi^0}$ requirements are estimated to be 0.9%, 1.8%, and 1.8% for $D^0 \rightarrow K^- \eta e^+ \nu_e$, $D^+ \rightarrow K_S^0 \eta e^+ \nu_e$ and $D^+ \rightarrow \eta \eta e^+ \nu_e$ decays, respectively, and are estimated using DT samples of $D^0 \rightarrow K^- e^+ \nu_e$ and $D^+ \rightarrow K_S^0 e^+ \nu_e$ decays reconstructed versus the same tags as the default analysis. The systematic uncertainties from the $M_{P\eta e^+}$ requirements are estimated to be 1.7%, 2.7%, and 2.7% for $D^0 \rightarrow K^- \eta e^+ \nu_e$, $D^+ \rightarrow K_S^0 \eta e^+ \nu_e$ and $D^+ \rightarrow \eta \eta e^+ \nu_e$, respectively, which are estimated using DT samples of $D^0 \rightarrow K^- \pi^0 e^+ \nu_e$ and $D^+ \rightarrow K_S^0 \pi^0 e^+ \nu_e$ decays reconstructed versus the same tags as the default analysis.

The contribution of the $M_{K-\eta}$ requirement to the systematic uncertainty is found to be negligible.

The systematic uncertainty related to the MC generator is estimated using alternative signal MC samples, where the ISGW2 model is replaced by a PHSP model for $D \rightarrow \mathcal{R} e^+ \nu_e$. The changes of the signal efficiencies, 1.9%, 0.1%, and 0.1%, are taken as the systematic uncertainties for $D^0 \rightarrow K^- \eta e^+ \nu_e$, $D^+ \rightarrow K_S^0 \eta e^+ \nu_e$ and $D^+ \rightarrow \eta \eta e^+ \nu_e$, respectively. The systematic uncertainty of the MC generator is also considered by varying the mass and width of the assumed resonances according individual PDG values [14]. The changes of the signal efficiencies, 7.9%, 6.0%, and 6.3%, are taken as the systematic uncertainties for $D^0 \rightarrow K^- \eta e^+ \nu_e$, $D^+ \rightarrow K_S^0 \eta e^+ \nu_e$, and $D^+ \rightarrow \eta \eta e^+ \nu_e$, respectively. The systematic uncertainties due to unknown resonance are assigned as the differences between the nominal efficiencies and those obtained with ISGW2 or PHSP models, which are 24.4%, 17.0%, and 36.4% for $D^0 \rightarrow K^- \eta e^+ \nu_e$, $D^+ \rightarrow K_S^0 \eta e^+ \nu_e$ and $D^+ \rightarrow \eta \eta e^+ \nu_e$, respectively. Additionally, the uncertainties due to the limited MC sample size, propagated from DT efficiencies, are 0.5%, 0.4%, and 0.5% for $D^0 \rightarrow K^- \eta e^+ \nu_e$, $D^+ \rightarrow K_S^0 \eta e^+ \nu_e$ and $D^+ \rightarrow \eta \eta e^+ \nu_e$, respectively.

By summing these uncertainties in quadrature, the total systematic uncertainties associated with the signal efficiencies, σ_e , are determined to be 26.0% assumption for $D^0 \rightarrow K^- \eta e^+ \nu_e$, 18.5% for $D^+ \rightarrow K_S^0 \eta e^+ \nu_e$, and 37.2% for $D^+ \rightarrow \eta \eta e^+ \nu_e$, respectively. These systematic uncertainties are summarized in Table III.

The additive systematic uncertainties originate from the fits to the U_{miss} distributions of the semileptonic D decay candidates. They are dominated by the uncertainty from the background shape. This systematic uncertainty is studied by altering the default MC background shape with two methods. First, alternative MC samples are used to

TABLE III. Systematic uncertainties in % for the branching fractions and upper limits, where the dash (—) indicates a systematic effect is not applicable.

Source	$D^0 \rightarrow K^- \eta e^+ \nu_e$	$D^+ \rightarrow K_S^0 \eta e^+ \nu_e$	$D^+ \rightarrow \eta \eta e^+ \nu_e$
N_{tag}	0.1	0.1	0.1
K^-, e^+ tracking	2.0	1.0	1.0
K^-, e^+ PID	2.0	1.0	1.0
η reconstruction	1.0	1.0	2.0
K_S^0 reconstruction	—	1.7	—
$E_{\text{extray}}^{\text{max}}$, $N_{\text{extra}}^{\text{char}}$, and $N_{\text{extra}}^{\pi^0}$ requirements	0.9	1.8	1.8
$M_{\eta P e^+}$ requirement	1.7	2.7	2.7
Daughter branching fractions	0.5	0.5	0.9
MC sample size	0.5	0.4	0.5
MC model	8.1	6.0	6.3
Unknown resonance	24.4	17.0	36.4
U_{miss} fit	0.3	—	—
Total	26.0	18.5	37.2

TABLE IV. The signal yields ($N_{\text{sig}}^{\text{fit}}$), the statistical significances, the signal efficiencies ($\bar{\epsilon}_{\text{SL}}$), the branching fractions (\mathcal{B}), the upper limits on the accepted events ($N_{\text{sig}}^{\text{up}}$), and the upper limits of the branching fractions at the 90% confidence level, (\mathcal{B}^{up}) for $D^0 \rightarrow K^-\eta e^+\nu_e$, $D^+ \rightarrow K_S^0\eta e^+\nu_e$ and $D^+ \rightarrow \eta\eta e^+\nu_e$ decays.

Decay	$N_{\text{sig}}^{\text{fit}}$	Significance (σ)	$N_{\text{sig}}^{\text{up}}$	$\bar{\epsilon}_{\text{SL}}(\%)$	$\mathcal{B}(\times 10^{-4})$	$\mathcal{B}^{\text{up}}(\times 10^{-4})$
$D^0 \rightarrow K^-\eta e^+\nu_e$	$11.1_{-3.8}^{+4.5}$	3.3	...	5.29 ± 0.05	$0.84_{-0.29}^{+0.34} \pm 0.22$...
$D^+ \rightarrow K_S^0\eta e^+\nu_e$	$8.4_{-3.9}^{+4.7}$	1.9	17.8	7.79 ± 0.05	...	<2.0
$D^+ \rightarrow \eta\eta e^+\nu_e$	$0.3_{-1.2}^{+1.9}$	0.0	4.8	7.52 ± 0.05	...	<1.0

determine the background shape, where the relative fractions of the $q\bar{q}$ background is varied within the uncertainties. Second, the branching fractions of the major $D\bar{D}$ background sources. $D^0 \rightarrow K^-\pi^+\pi^0\pi^0$, $D^0 \rightarrow K^-\pi^0 e^+\nu_e$, $D^0 \rightarrow K^-\pi^+\eta$, $D^+ \rightarrow K_S^0\pi^0 e^+\nu_e$, $D^+ \rightarrow K_S^0\pi^+\eta$, $D^+ \rightarrow K_S^0\pi^+\pi^0\pi^0$, $D^+ \rightarrow K_S^0\pi^0 e^+\nu_e$, $D^+ \rightarrow K_S^0 e^+\nu_e$, and $D^+ \rightarrow K_S^0\pi^0\pi^+$ are varied within their uncertainties [14]. The signal shape is varied from the MC simulated shape to an analytical shape described by a double-Gaussian function, with the means, widths, and relative areas of the two Gaussian components fixed from a fit to the signal MC sample. The uncertainty associated with the fit to the U_{miss} distribution is estimated to be 0.3% for the $D^0 \rightarrow K^-\eta e^+\nu_e$ decay, and is also summarized in Table III. The additive systematic uncertainties for $D^+ \rightarrow K_S^0\eta e^+\nu_e$ and $D^+ \rightarrow \eta\eta e^+\nu_e$ are considered in the maximum-likelihood results in next section.

VII. RESULTS

To take into account the additive systematic uncertainty in the limits, the maximum-likelihood fits are repeated using different alternative background shapes as mentioned in the previous section and the one resulting in the most conservative upper limit is chosen. To incorporate the multiplicative systematic uncertainties in the calculation of the upper limits, the likelihood distribution is smeared by a Gaussian function with a mean of zero and a width equal to σ_ϵ [23]

$$L(\mathcal{B}) \propto \int_0^1 L\left(\mathcal{B}\frac{\epsilon}{\epsilon_0}\right) e^{-\frac{(\epsilon-\epsilon_0)^2}{2\sigma_\epsilon^2}} d\epsilon, \quad (2)$$

where $L(\mathcal{B})$ is the likelihood distribution as a function of assumed branching fractions, ϵ is the expected efficiency and ϵ_0 is the average MC-estimated efficiency.

The red solid curves in Fig. 4 show the likelihood distributions incorporating the systematic uncertainties for $D^+ \rightarrow K_S^0\eta e^+\nu_e$ and $D^+ \rightarrow \eta\eta e^+\nu_e$ decays, respectively. The upper limits on the product of branching fractions of $D^+ \rightarrow K_S^0\eta e^+\nu_e$ and $D^+ \rightarrow \eta\eta e^+\nu_e$ at the 90% CL are 2.0×10^{-4} and 1.0×10^{-4} , respectively.

Finally, we note that the additive systematic does not affect the significance of the $D^0 \rightarrow K^-\eta e^+\nu_e$ mode within the quoted precision.

VIII. SUMMARY

Based on a 7.93 fb^{-1} sample of e^+e^- collision data taken at $\sqrt{s} = 3.773 \text{ GeV}$ with the BESIII detector, the semi-leptonic decays $D^0 \rightarrow K^-\eta e^+\nu_e$, $D^+ \rightarrow K_S^0\eta e^+\nu_e$ and $D^+ \rightarrow \eta\eta e^+\nu_e$ have been investigated for the first time. Evidence for $D^0 \rightarrow K^-\eta e^+\nu_e$ is found with a significance of 3.3σ . The branching fraction of $D^0 \rightarrow K^-\eta e^+\nu_e$ is determined to be $(0.84_{-0.34}^{+0.29} \pm 0.22) \times 10^{-4}$. No significant signals are found for $D^+ \rightarrow K_S^0\eta e^+\nu_e$ and $D^+ \rightarrow \eta\eta e^+\nu_e$ and the upper limits on their branching fractions are set at the 90% CL. With the currently available data sample, the obtained upper limits are comparable with the theoretical calculations. The detailed results are presented in Table IV.

ACKNOWLEDGMENTS

The BESIII Collaboration thanks the staff of BEPCII and the IHEP computing center for their strong support. This work is supported in part by National Key R&D Program of China under Contracts No. 2023YFA1606000, No. 2020YFA0406400, No. 2020YFA0406300; National Natural Science Foundation of China (NSFC) under Contracts No. 11635010, No. 11735014, No. 11935015, No. 11935016, No. 11935018, No. 12025502, No. 12035009, No. 12035013, No. 12061131003, No. 12192260, No. 12192261, No. 12192262, No. 12192263, No. 12192264, No. 12192265, No. 12221005, No. 12225509, No. 12235017, No. 12361141819; the Chinese Academy of Sciences (CAS) Large-Scale Scientific Facility Program; the CAS Center for Excellence in Particle Physics (CCEPP); Joint Large-Scale Scientific Facility Funds of the NSFC and CAS under Contract No. U1832207; 100 Talents Program of CAS; The Institute of Nuclear and Particle Physics (INPAC) and Shanghai Key Laboratory for Particle Physics and Cosmology; German Research Foundation DFG under Contracts Nos. 455635585, FOR5327, GRK 2149; Istituto Nazionale di Fisica Nucleare, Italy; Ministry of Development of Turkey under Contract No. DPT2006K-

120470; National Research Foundation of Korea under Contract No. NRF-2022R1A2C1092335; National Science and Technology fund of Mongolia; National Science Research and Innovation Fund (NSRF) via the Program Management Unit for Human Resources & Institutional Development, Research and Innovation of Thailand under Contract No. B16F640076; Polish National Science Centre

under Contract No. 2019/35/O/ST2/02907; The Swedish Research Council; U.S. Department of Energy under Contract No. DE-FG02-05ER41374.

DATA AVAILABILITY

No data were created or analyzed in this study.

-
- [1] B. C. Ke, J. Koponen, H. B. Li, and Y. Zheng, *Annu. Rev. Nucl. Part. Sci.* **73**, 285 (2023).
 [2] W. Wang and C. D. Lu, *Phys. Rev. D* **82**, 034016 (2010).
 [3] N. N. Achasov and A. V. Kiselev, *Phys. Rev. D* **86**, 114010 (2012).
 [4] E. Oset, W. H. Liang, M. Bayar, J. J. Xie, L. R. Dai, M. Albaladejo, M. Nielsen, T. Sekihara, F. Navarra, L. Roca *et al.*, *Int. J. Mod. Phys. E* **25**, 1630001 (2016).
 [5] R. M. Wang, Y. Qiao, Y. J. Zhang, X. D. Cheng, and Y. G. Xu, *Phys. Rev. D* **107**, 056022 (2023).
 [6] H. Y. Cheng and X. W. Kang, *Eur. Phys. J. C* **77**, 587 (2017); **77**, 863(E) (2017).
 [7] M. Ablikim *et al.* (BESIII Collaboration), *Nucl. Instrum. Methods Phys. Res., Sect. A* **614**, 345 (2010).
 [8] C. Yu *et al.*, *Proceedings of the 7th International Particle Accelerator Conference* (2016), p. TUYA01, 10.18429/JACoW-IPAC2016-TUYA01.
 [9] S. Agostinelli *et al.* (GEANT4 Collaboration), *Nucl. Instrum. Methods Phys. Res., Sect. A* **506**, 250 (2003).
 [10] S. Jadach, B. F. L. Ward, and Z. Was, *Comput. Phys. Commun.* **130**, 260 (2000).
 [11] S. Jadach, B. F. L. Ward, and Z. Was, *Phys. Rev. D* **63**, 113009 (2001).
 [12] R. G. Ping, *Chin. Phys. C* **32**, 599 (2008).
 [13] D. J. Lange, *Nucl. Instrum. Methods Phys. Res., Sect. A* **462**, 152 (2001).
 [14] R. L. Workman *et al.* (Particle Data Group), *Prog. Theor. Exp. Phys.* **2022**, 083C01 (2022).
 [15] J. C. Chen, G. S. Huang, X. R. Qi, D. H. Zhang, and Y. S. Zhu, *Phys. Rev. D* **62**, 034003 (2000).
 [16] E. Richter-Was, *Phys. Lett. B* **303**, 163 (1993).
 [17] D. Scora and N. Isgur, *Phys. Rev. D* **52**, 2783 (1995).
 [18] R. M. Baltrusaitis *et al.* (MARK-III Collaboration), *Phys. Rev. Lett.* **56**, 2140 (1986).
 [19] J. Adler *et al.* (MARK-III Collaboration), *Phys. Rev. Lett.* **60**, 89 (1988).
 [20] M. Ablikim *et al.* (BESIII Collaboration), *Phys. Lett. B* **734**, 227 (2014).
 [21] H. Albrecht *et al.* (ARGUS Collaboration), *Phys. Lett. B* **241**, 278 (1990).
 [22] M. Ablikim *et al.* (BESIII Collaboration), *Phys. Rev. D* **104**, 052008 (2021).
 [23] K. Stenson, arXiv:physics/0605236.

M. Ablikim,¹ M. N. Achasov,^{4,c} P. Adlarson,⁷⁵ O. Afedulidis,³ X. C. Ai,⁸⁰ R. Aliberti,³⁵ A. Amoroso,^{74a,74c} Q. An,^{71,58,a} Y. Bai,⁵⁷ O. Bakina,³⁶ I. Balossino,^{29a} Y. Ban,^{46,h} H.-R. Bao,⁶³ V. Batozskaya,^{1,44} K. Begzsuren,³² N. Berger,³⁵ M. Berlowski,⁴⁴ M. Bertani,^{28a} D. Bettoni,^{29a} F. Bianchi,^{74a,74c} E. Bianco,^{74a,74c} A. Bortone,^{74a,74c} I. Boyko,³⁶ R. A. Briere,⁵ A. Brueggemann,⁶⁸ H. Cai,⁷⁶ X. Cai,^{1,58} A. Calcaterra,^{28a} G. F. Cao,^{1,63} N. Cao,^{1,63} S. A. Cetin,^{62a} J. F. Chang,^{1,58} G. R. Che,⁴³ G. Chelkov,^{36,b} C. Chen,⁴³ C. H. Chen,⁹ Chao Chen,⁵⁵ G. Chen,¹ H. S. Chen,^{1,63} H. Y. Chen,²⁰ M. L. Chen,^{1,58,63} S. J. Chen,⁴² S. L. Chen,⁴⁵ S. M. Chen,⁶¹ T. Chen,^{1,63} X. R. Chen,^{31,63} X. T. Chen,^{1,63} Y. B. Chen,^{1,58} Y. Q. Chen,³⁴ Z. J. Chen,^{25,i} Z. Y. Chen,^{1,63} S. K. Choi,¹⁰ G. Cibinetto,^{29a} F. Cossio,^{74c} J. J. Cui,⁵⁰ H. L. Dai,^{1,58} J. P. Dai,⁷⁸ A. Dbeyssi,¹⁸ R. E. de Boer,³ D. Dedovich,³⁶ C. Q. Deng,⁷² Z. Y. Deng,¹ A. Denig,³⁵ I. Denysenko,³⁶ M. Destefanis,^{74a,74c} F. De Mori,^{74a,74c} B. Ding,^{66,1} X. X. Ding,^{46,h} Y. Ding,³⁴ Y. Ding,⁴⁰ J. Dong,^{1,58} L. Y. Dong,^{1,63} M. Y. Dong,^{1,58,63} X. Dong,⁷⁶ M. C. Du,¹ S. X. Du,⁸⁰ Y. Y. Duan,⁵⁵ Z. H. Duan,⁴² P. Egorov,^{36,b} Y. H. Fan,⁴⁵ J. Fang,⁵⁹ J. Fang,^{1,58} S. S. Fang,^{1,63} W. X. Fang,¹ Y. Fang,¹ Y. Q. Fang,^{1,58} R. Farinelli,^{29a} L. Fava,^{74b,74c} F. Feldbauer,³ G. Felici,^{28a} C. Q. Feng,^{71,58} J. H. Feng,⁵⁹ Y. T. Feng,^{71,58} M. Fritsch,³ C. D. Fu,¹ J. L. Fu,⁶³ Y. W. Fu,^{1,63} H. Gao,⁶³ X. B. Gao,⁴¹ Y. N. Gao,^{46,h} Yang Gao,^{71,58} S. Garbolino,^{74c} I. Garzia,^{29a,29b} L. Ge,⁸⁰ P. T. Ge,⁷⁶ Z. W. Ge,⁴² C. Geng,⁵⁹ E. M. Gersabeck,⁶⁷ A. Gilman,⁶⁹ K. Goetzen,¹³ L. Gong,⁴⁰ W. X. Gong,^{1,58} W. Gradl,³⁵ S. Gramigna,^{29a,29b} M. Greco,^{74a,74c} M. H. Gu,^{1,58} Y. T. Gu,¹⁵ C. Y. Guan,^{1,63} A. Q. Guo,^{31,63} L. B. Guo,⁴¹ M. J. Guo,⁵⁰ R. P. Guo,⁴⁹ Y. P. Guo,^{12,g} A. Guskov,^{36,b} J. Gutierrez,²⁷ K. L. Han,⁶³ T. T. Han,¹ F. Hanisch,³ X. Q. Hao,¹⁹ F. A. Harris,⁶⁵ K. K. He,⁵⁵ K. L. He,^{1,63} F. H. Heinsius,³ C. H. Heinz,³⁵ Y. K. Heng,^{1,58,63}

C. Herold,⁶⁰ T. Holtmann,³ P. C. Hong,³⁴ G. Y. Hou,^{1,63} X. T. Hou,^{1,63} Y. R. Hou,⁶³ Z. L. Hou,¹ B. Y. Hu,⁵⁹ H. M. Hu,^{1,63} J. F. Hu,^{56,j} S. L. Hu,^{12,g} T. Hu,^{1,58,63} Y. Hu,¹ G. S. Huang,^{71,58} K. X. Huang,⁵⁹ L. Q. Huang,^{31,63} X. T. Huang,⁵⁰ Y. P. Huang,¹ Y. S. Huang,⁵⁹ T. Hussain,⁷³ F. Hölzken,³ N. Hüsken,³⁵ N. in der Wiesche,⁶⁸ J. Jackson,²⁷ S. Janchiv,³² J. H. Jeong,¹⁰ Q. Ji,¹ Q. P. Ji,¹⁹ W. Ji,^{1,63} X. B. Ji,^{1,63} X. L. Ji,^{1,58} Y. Y. Ji,⁵⁰ X. Q. Jia,⁵⁰ Z. K. Jia,^{71,58} D. Jiang,^{1,63} H. B. Jiang,⁷⁶ P. C. Jiang,^{46,h} S. S. Jiang,³⁹ T. J. Jiang,¹⁶ X. S. Jiang,^{1,58,63} Y. Jiang,⁶³ J. B. Jiao,⁵⁰ J. K. Jiao,³⁴ Z. Jiao,²³ S. Jin,⁴² Y. Jin,⁶⁶ M. Q. Jing,^{1,63} X. M. Jing,⁶³ T. Johansson,⁷⁵ S. Kabana,³³ N. Kalantar-Nayestanaki,⁶⁴ X. L. Kang,⁹ X. S. Kang,⁴⁰ M. Kavatsyuk,⁶⁴ B. C. Ke,⁸⁰ V. Khachatryan,²⁷ A. Khoukaz,⁶⁸ R. Kiuchi,¹ O. B. Kolcu,^{62a} B. Kopf,³ M. Kuessner,³ X. Kui,^{1,63} N. Kumar,²⁶ A. Kupsc,^{44,75} W. Kühn,³⁷ J. J. Lane,⁶⁷ L. Lavezzi,^{74a,74c} T. T. Lei,^{71,58} Z. H. Lei,^{71,58} M. Lellmann,³⁵ T. Lenz,³⁵ C. Li,⁴⁷ C. Li,⁴³ C. H. Li,³⁹ Cheng Li,^{71,58} D. M. Li,⁸⁰ F. Li,^{1,58} G. Li,¹ H. B. Li,^{1,63} H. J. Li,¹⁹ H. N. Li,^{56,j} Hui Li,⁴³ J. R. Li,⁶¹ J. S. Li,⁵⁹ K. Li,¹ L. J. Li,^{1,63} L. K. Li,¹ Lei Li,⁴⁸ M. H. Li,⁴³ P. R. Li,^{38,k,l} Q. M. Li,^{1,63} Q. X. Li,⁵⁰ R. Li,^{17,31} S. X. Li,¹² T. Li,⁵⁰ W. D. Li,^{1,63} W. G. Li,^{1,a} X. Li,^{1,63} X. H. Li,^{71,58} X. L. Li,⁵⁰ X. Y. Li,^{1,63} X. Z. Li,⁵⁹ Y. G. Li,^{46,h} Z. J. Li,⁵⁹ Z. Y. Li,⁷⁸ C. Liang,⁴² H. Liang,^{1,63} H. Liang,^{71,58} Y. F. Liang,⁵⁴ Y. T. Liang,^{31,63} G. R. Liao,¹⁴ Y. P. Liao,^{1,63} J. Libby,²⁶ A. Limphirat,⁶⁰ C. C. Lin,⁵⁵ D. X. Lin,^{31,63} T. Lin,¹ B. J. Liu,¹ B. X. Liu,⁷⁶ C. Liu,³⁴ C. X. Liu,¹ F. Liu,¹ F. H. Liu,⁵³ Feng Liu,⁶ G. M. Liu,^{56,j} H. Liu,^{38,k,l} H. B. Liu,¹⁵ H. H. Liu,¹ H. M. Liu,^{1,63} Huihui Liu,²¹ J. B. Liu,^{71,58} J. Y. Liu,^{1,63} K. Liu,^{38,k,l} K. Y. Liu,⁴⁰ Ke Liu,²² L. Liu,^{71,58} L. C. Liu,⁴³ Lu Liu,⁴³ M. H. Liu,^{12,g} P. L. Liu,¹ Q. Liu,⁶³ S. B. Liu,^{71,58} T. Liu,^{12,g} W. K. Liu,⁴³ W. M. Liu,^{71,58} X. Liu,^{38,k,l} X. Liu,³⁹ Y. Liu,⁸⁰ Y. Liu,^{38,k,l} Y. B. Liu,⁴³ Z. A. Liu,^{1,58,63} Z. D. Liu,⁹ Z. Q. Liu,⁵⁰ X. C. Lou,^{1,58,63} F. X. Lu,⁵⁹ H. J. Lu,²³ J. G. Lu,^{1,58} X. L. Lu,¹ Y. Lu,⁷ Y. P. Lu,^{1,58} Z. H. Lu,^{1,63} C. L. Luo,⁴¹ J. R. Luo,⁵⁹ M. X. Luo,⁷⁹ T. Luo,^{12,g} X. L. Luo,^{1,58} X. R. Lyu,⁶³ Y. F. Lyu,⁴³ F. C. Ma,⁴⁰ H. Ma,⁷⁸ H. L. Ma,¹ J. L. Ma,^{1,63} L. L. Ma,⁵⁰ M. M. Ma,^{1,63} Q. M. Ma,¹ R. Q. Ma,^{1,63} T. Ma,^{71,58} X. T. Ma,^{1,63} X. Y. Ma,^{1,58} Y. Ma,^{46,h} Y. M. Ma,³¹ F. E. Maas,¹⁸ M. Maggiora,^{74a,74c} S. Malde,⁶⁹ Y. J. Mao,^{46,h} Z. P. Mao,¹ S. Marcello,^{74a,74c} Z. X. Meng,⁶⁶ J. G. Messchendorp,^{13,64} G. Mezzadri,^{29a} H. Miao,^{1,63} T. J. Min,⁴² R. E. Mitchell,²⁷ X. H. Mo,^{1,58,63} B. Moses,²⁷ N. Yu. Muchnoi,^{4,c} J. Muskalla,³⁵ Y. Nefedov,³⁶ F. Nerling,^{18,e} L. S. Nie,²⁰ I. B. Nikolaev,^{4,c} Z. Ning,^{1,58} S. Nisar,^{11,m} Q. L. Niu,^{38,k,l} W. D. Niu,⁵⁵ Y. Niu,⁵⁰ S. L. Olsen,⁶³ Q. Ouyang,^{1,58,63} S. Pacetti,^{28b,28c} X. Pan,⁵⁵ Y. Pan,⁵⁷ A. Pathak,³⁴ Y. P. Pei,^{71,58} M. Pelizaesus,³ H. P. Peng,^{71,58} Y. Y. Peng,^{38,k,l} K. Peters,^{13,e} J. L. Ping,⁴¹ R. G. Ping,^{1,63} S. Plura,³⁵ V. Prasad,³³ F. Z. Qi,¹ H. Qi,^{71,58} H. R. Qi,⁶¹ M. Qi,⁴² T. Y. Qi,^{12,g} S. Qian,^{1,58} W. B. Qian,⁶³ C. F. Qiao,⁶³ X. K. Qiao,⁸⁰ J. J. Qin,⁷² L. Q. Qin,¹⁴ L. Y. Qin,^{71,58} X. P. Qin,^{12,g} X. S. Qin,⁵⁰ Z. H. Qin,^{1,58} J. F. Qiu,¹ Z. H. Qu,⁷² C. F. Redmer,³⁵ K. J. Ren,³⁹ A. Rivetti,^{74c} M. Rolo,^{74c} G. Rong,^{1,63} Ch. Rosner,¹⁸ S. N. Ruan,⁴³ N. Salone,⁴⁴ A. Sarantsev,^{36,d} Y. Schelhaas,³⁵ K. Schoenning,⁷⁵ M. Scodreggio,^{29a} K. Y. Shan,^{12,g} W. Shan,²⁴ X. Y. Shan,^{71,58} Z. J. Shang,^{38,k,l} J. F. Shangguan,¹⁶ L. G. Shao,^{1,63} M. Shao,^{71,58} C. P. Shen,^{12,g} H. F. Shen,^{1,8} W. H. Shen,⁶³ X. Y. Shen,^{1,63} B. A. Shi,⁶³ H. Shi,^{71,58} H. C. Shi,^{71,58} J. L. Shi,^{12,g} J. Y. Shi,¹ Q. Q. Shi,⁵⁵ S. Y. Shi,⁷² X. Shi,^{1,58} J. J. Song,¹⁹ T. Z. Song,⁵⁹ W. M. Song,^{34,1} Y. J. Song,^{12,g} Y. X. Song,^{46,h,n} S. Sosio,^{74a,74c} S. Spataro,^{74a,74c} F. Stieler,³⁵ Y. J. Su,⁶³ G. B. Sun,⁷⁶ G. X. Sun,¹ H. Sun,⁶³ H. K. Sun,¹ J. F. Sun,¹⁹ K. Sun,⁶¹ L. Sun,⁷⁶ S. S. Sun,^{1,63} T. Sun,^{51,f} W. Y. Sun,³⁴ Y. Sun,⁹ Y. J. Sun,^{71,58} Y. Z. Sun,¹ Z. Q. Sun,^{1,63} Z. T. Sun,⁵⁰ C. J. Tang,⁵⁴ G. Y. Tang,¹ J. Tang,⁵⁹ M. Tang,^{71,58} Y. A. Tang,⁷⁶ L. Y. Tao,⁷² Q. T. Tao,^{25,i} M. Tat,⁶⁹ J. X. Teng,^{71,58} V. Thoren,⁷⁵ W. H. Tian,⁵⁹ Y. Tian,^{31,63} Z. F. Tian,⁷⁶ I. Uman,^{62b} Y. Wan,⁵⁵ S. J. Wang,⁵⁰ B. Wang,¹ B. L. Wang,⁶³ Bo Wang,^{71,58} D. Y. Wang,^{46,h} F. Wang,⁷² H. J. Wang,^{38,k,l} J. J. Wang,⁷⁶ J. P. Wang,⁵⁰ K. Wang,^{1,58} L. L. Wang,¹ M. Wang,⁵⁰ N. Y. Wang,⁶³ S. Wang,^{12,g} S. Wang,^{38,k,l} T. Wang,^{12,g} T. J. Wang,⁴³ W. Wang,⁵⁹ W. Wang,⁷² W. P. Wang,^{35,71,o} X. Wang,^{46,h} X. F. Wang,^{38,k,l} X. J. Wang,³⁹ X. L. Wang,^{12,g} X. N. Wang,¹ Y. Wang,⁶¹ Y. D. Wang,⁴⁵ Y. F. Wang,^{1,58,63} Y. L. Wang,¹⁹ Y. N. Wang,⁴⁵ Y. Q. Wang,¹ Yaqian Wang,¹⁷ Yi Wang,⁶¹ Z. Wang,^{1,58} Z. L. Wang,⁷² Z. Y. Wang,^{1,63} Ziyi Wang,⁶³ D. H. Wei,¹⁴ F. Weidner,⁶⁸ S. P. Wen,¹ Y. R. Wen,³⁹ U. Wiedner,³ G. Wilkinson,⁶⁹ M. Wolke,⁷⁵ L. Wollenberg,³ C. Wu,³⁹ J. F. Wu,^{1,8} L. H. Wu,¹ L. J. Wu,^{1,63} X. Wu,^{12,g} X. H. Wu,³⁴ Y. Wu,^{71,58} Y. H. Wu,⁵⁵ Y. J. Wu,³¹ Z. Wu,^{1,58} L. Xia,^{71,58} X. M. Xian,³⁹ B. H. Xiang,^{1,63} T. Xiang,^{46,h} D. Xiao,^{38,k,l} G. Y. Xiao,⁴² S. Y. Xiao,¹ Y. L. Xiao,^{12,g} Z. J. Xiao,⁴¹ C. Xie,⁴² X. H. Xie,^{46,h} Y. Xie,⁵⁰ Y. G. Xie,^{1,58} Y. H. Xie,⁶ Z. P. Xie,^{71,58} T. Y. Xing,^{1,63} C. F. Xu,^{1,63} C. J. Xu,⁵⁹ G. F. Xu,¹ H. Y. Xu,^{66,2,p} M. Xu,^{71,58} Q. J. Xu,¹⁶ Q. N. Xu,³⁰ W. Xu,¹ W. L. Xu,⁶⁶ X. P. Xu,⁵⁵ Y. C. Xu,⁷⁷ Z. S. Xu,⁶³ F. Yan,^{12,g} L. Yan,^{12,g} W. B. Yan,^{71,58} W. C. Yan,⁸⁰ X. Q. Yan,¹ H. J. Yang,^{51,f} H. L. Yang,³⁴ H. X. Yang,¹ T. Yang,¹ Y. Yang,^{12,g} Y. F. Yang,^{1,63} Y. F. Yang,⁴³ Y. X. Yang,^{1,63} Z. W. Yang,^{38,k,l} Z. P. Yao,⁵⁰ M. Ye,^{1,58} M. H. Ye,⁸ J. H. Yin,¹ Z. Y. You,⁵⁹ B. X. Yu,^{1,58,63} C. X. Yu,⁴³ G. Yu,^{1,63} J. S. Yu,^{25,i} T. Yu,⁷² X. D. Yu,^{46,h} Y. C. Yu,⁸⁰ C. Z. Yuan,^{1,63} J. Yuan,³⁴ J. Yuan,⁴⁵ L. Yuan,² S. C. Yuan,^{1,63} Y. Yuan,^{1,63} Z. Y. Yuan,⁵⁹ C. X. Yue,³⁹ A. A. Zafar,⁷³ F. R. Zeng,⁵⁰ S. H. Zeng,⁷² X. Zeng,^{12,g} Y. Zeng,^{25,i} Y. J. Zeng,⁵⁹ Y. J. Zeng,^{1,63} X. Y. Zhai,³⁴ Y. C. Zhai,⁵⁰ Y. H. Zhan,⁵⁹ A. Q. Zhang,^{1,63} B. L. Zhang,^{1,63} B. X. Zhang,¹ D. H. Zhang,⁴³ G. Y. Zhang,¹⁹ H. Zhang,⁸⁰ H. Zhang,^{71,58} H. C. Zhang,^{1,58,63} H. H. Zhang,³⁴ H. H. Zhang,⁵⁹ H. Q. Zhang,^{1,58,63} H. R. Zhang,^{71,58} H. Y. Zhang,^{1,58} J. Zhang,⁸⁰ J. Zhang,⁵⁹ J. J. Zhang,⁵²

J. L. Zhang,²⁰ J. Q. Zhang,⁴¹ J. S. Zhang,^{12,g} J. W. Zhang,^{1,58,63} J. X. Zhang,^{38,k,l} J. Y. Zhang,¹ J. Z. Zhang,^{1,63}
 Jianyu Zhang,⁶³ L. M. Zhang,⁶¹ Lei Zhang,⁴² P. Zhang,^{1,63} Q. Y. Zhang,³⁴ R. Y. Zhang,^{38,k,l} S. H. Zhang,^{1,63} Shulei Zhang,^{25,i}
 X. D. Zhang,⁴⁵ X. M. Zhang,¹ X. Y. Zhang,⁵⁰ Y. Zhang,⁷² Y. Zhang,¹ Y. T. Zhang,⁸⁰ Y. H. Zhang,^{1,58} Y. M. Zhang,³⁹
 Yan Zhang,^{71,58} Z. D. Zhang,¹ Z. H. Zhang,¹ Z. L. Zhang,³⁴ Z. Y. Zhang,⁷⁶ Z. Y. Zhang,⁴³ Z. Z. Zhang,⁴⁵ G. Zhao,¹
 J. Y. Zhao,^{1,63} J. Z. Zhao,^{1,58} L. Zhao,¹ Lei Zhao,^{71,58} M. G. Zhao,⁴³ N. Zhao,⁷⁸ R. P. Zhao,⁶³ S. J. Zhao,⁸⁰ Y. B. Zhao,^{1,58}
 Y. X. Zhao,^{31,63} Z. G. Zhao,^{71,58} A. Zhemchugov,^{36,b} B. Zheng,⁷² B. M. Zheng,³⁴ J. P. Zheng,^{1,58} W. J. Zheng,^{1,63}
 Y. H. Zheng,⁶³ B. Zhong,⁴¹ X. Zhong,⁵⁹ H. Zhou,⁵⁰ J. Y. Zhou,³⁴ L. P. Zhou,^{1,63} S. Zhou,⁶ X. Zhou,⁷⁶ X. K. Zhou,⁶
 X. R. Zhou,^{71,58} X. Y. Zhou,³⁹ Y. Z. Zhou,^{12,g} J. Zhu,⁴³ K. Zhu,¹ K. J. Zhu,^{1,58,63} K. S. Zhu,^{12,g} L. Zhu,³⁴ L. X. Zhu,⁶³
 S. H. Zhu,⁷⁰ T. J. Zhu,^{12,g} W. D. Zhu,⁴¹ Y. C. Zhu,^{71,58} Z. A. Zhu,^{1,63} J. H. Zou,¹ and J. Zu^{71,58}

(BESIII Collaboration)

¹*Institute of High Energy Physics, Beijing 100049, People's Republic of China*

²*Beihang University, Beijing 100191, People's Republic of China*

³*Bochum Ruhr-University, D-44780 Bochum, Germany*

⁴*Budker Institute of Nuclear Physics SB RAS (BINP), Novosibirsk 630090, Russia*

⁵*Carnegie Mellon University, Pittsburgh, Pennsylvania 15213, USA*

⁶*Central China Normal University, Wuhan 430079, People's Republic of China*

⁷*Central South University, Changsha 410083, People's Republic of China*

⁸*China Center of Advanced Science and Technology, Beijing 100190, People's Republic of China*

⁹*China University of Geosciences, Wuhan 430074, People's Republic of China*

¹⁰*Chung-Ang University, Seoul, 06974, Republic of Korea*

¹¹*COMSATS University Islamabad, Lahore Campus, Defence Road, Off Raiwind Road, 54000 Lahore, Pakistan*

¹²*Fudan University, Shanghai 200433, People's Republic of China*

¹³*GSI Helmholtzcentre for Heavy Ion Research GmbH, D-64291 Darmstadt, Germany*

¹⁴*Guangxi Normal University, Guilin 541004, People's Republic of China*

¹⁵*Guangxi University, Nanning 530004, People's Republic of China*

¹⁶*Hangzhou Normal University, Hangzhou 310036, People's Republic of China*

¹⁷*Hebei University, Baoding 071002, People's Republic of China*

¹⁸*Helmholtz Institute Mainz, Staudinger Weg 18, D-55099 Mainz, Germany*

¹⁹*Henan Normal University, Xinxiang 453007, People's Republic of China*

²⁰*Henan University, Kaifeng 475004, People's Republic of China*

²¹*Henan University of Science and Technology, Luoyang 471003, People's Republic of China*

²²*Henan University of Technology, Zhengzhou 450001, People's Republic of China*

²³*Huangshan College, Huangshan 245000, People's Republic of China*

²⁴*Hunan Normal University, Changsha 410081, People's Republic of China*

²⁵*Hunan University, Changsha 410082, People's Republic of China*

²⁶*Indian Institute of Technology Madras, Chennai 600036, India*

²⁷*Indiana University, Bloomington, Indiana 47405, USA*

^{28a}*INFN Laboratori Nazionali di Frascati, INFN Laboratori Nazionali di Frascati, I-00044, Frascati, Italy*

^{28b}*INFN Sezione di Perugia, I-06100, Perugia, Italy*

^{28c}*University of Perugia, I-06100, Perugia, Italy*

^{29a}*INFN Sezione di Ferrara, INFN Sezione di Ferrara, I-44122 Ferrara, Italy*

^{29b}*University of Ferrara, I-44122 Ferrara, Italy*

³⁰*Inner Mongolia University, Hohhot 010021, People's Republic of China*

³¹*Institute of Modern Physics, Lanzhou 730000, People's Republic of China*

³²*Institute of Physics and Technology, Peace Avenue 54B, Ulaanbaatar 13330, Mongolia*

³³*Instituto de Alta Investigación, Universidad de Tarapacá, Casilla 7D, Arica 1000000, Chile*

³⁴*Jilin University, Changchun 130012, People's Republic of China*

³⁵*Johannes Gutenberg University of Mainz, Johann-Joachim-Becher-Weg 45, D-55099 Mainz, Germany*

³⁶*Joint Institute for Nuclear Research, 141980 Dubna, Moscow region, Russia*

³⁷*Justus-Liebig-Universitaet Giessen, II. Physikalisches Institut, Heinrich-Buff-Ring 16, D-35392 Giessen, Germany*

³⁸*Lanzhou University, Lanzhou 730000, People's Republic of China*

³⁹*Liaoning Normal University, Dalian 116029, People's Republic of China*

⁴⁰*Liaoning University, Shenyang 110036, People's Republic of China*

⁴¹*Nanjing Normal University, Nanjing 210023, People's Republic of China*

- ⁴²Nanjing University, Nanjing 210093, People's Republic of China
⁴³Nankai University, Tianjin 300071, People's Republic of China
⁴⁴National Centre for Nuclear Research, Warsaw 02-093, Poland
⁴⁵North China Electric Power University, Beijing 102206, People's Republic of China
⁴⁶Peking University, Beijing 100871, People's Republic of China
⁴⁷Qufu Normal University, Qufu 273165, People's Republic of China
⁴⁸Renmin University of China, Beijing 100872, People's Republic of China
⁴⁹Shandong Normal University, Jinan 250014, People's Republic of China
⁵⁰Shandong University, Jinan 250100, People's Republic of China
⁵¹Shanghai Jiao Tong University, Shanghai 200240, People's Republic of China
⁵²Shanxi Normal University, Linfen 041004, People's Republic of China
⁵³Shanxi University, Taiyuan 030006, People's Republic of China
⁵⁴Sichuan University, Chengdu 610064, People's Republic of China
⁵⁵Soochow University, Suzhou 215006, People's Republic of China
⁵⁶South China Normal University, Guangzhou 510006, People's Republic of China
⁵⁷Southeast University, Nanjing 211100, People's Republic of China
⁵⁸State Key Laboratory of Particle Detection and Electronics, Beijing 100049, Hefei 230026, People's Republic of China
⁵⁹Sun Yat-Sen University, Guangzhou 510275, People's Republic of China
⁶⁰Suranaree University of Technology, University Avenue 111, Nakhon Ratchasima 30000, Thailand
⁶¹Tsinghua University, Beijing 100084, People's Republic of China
^{62a}Turkish Accelerator Center Particle Factory Group, Istinye University, 34010, Istanbul, Turkey
^{62b}Near East University, Nicosia, North Cyprus, 99138, Mersin 10, Turkey
⁶³University of Chinese Academy of Sciences, Beijing 100049, People's Republic of China
⁶⁴University of Groningen, NL-9747 AA Groningen, The Netherlands
⁶⁵University of Hawaii, Honolulu, Hawaii 96822, USA
⁶⁶University of Jinan, Jinan 250022, People's Republic of China
⁶⁷University of Manchester, Oxford Road, Manchester, M13 9PL, United Kingdom
⁶⁸University of Muenster, Wilhelm-Klemm-Strasse 9, 48149 Muenster, Germany
⁶⁹University of Oxford, Keble Road, Oxford OX13RH, United Kingdom
⁷⁰University of Science and Technology Liaoning, Anshan 114051, People's Republic of China
⁷¹University of Science and Technology of China, Hefei 230026, People's Republic of China
⁷²University of South China, Hengyang 421001, People's Republic of China
⁷³University of the Punjab, Lahore-54590, Pakistan
^{74a}University of Turin and INFN, University of Turin, I-10125, Turin, Italy;
^{74b}University of Eastern Piedmont, I-15121, Alessandria, Italy
^{74c}INFN, I-10125, Turin, Italy
⁷⁵Uppsala University, Box 516, SE-75120 Uppsala, Sweden
⁷⁶Wuhan University, Wuhan 430072, People's Republic of China
⁷⁷Yantai University, Yantai 264005, People's Republic of China
⁷⁸Yunnan University, Kunming 650500, People's Republic of China
⁷⁹Zhejiang University, Hangzhou 310027, People's Republic of China
⁸⁰Zhengzhou University, Zhengzhou 450001, People's Republic of China

^aDeceased.

^bAlso at the Moscow Institute of Physics and Technology, Moscow 141700, Russia.

^cAlso at the Novosibirsk State University, Novosibirsk, 630090, Russia.

^dAlso at the NRC "Kurchatov Institute", PNPI, 188300, Gatchina, Russia.

^eAlso at Goethe University Frankfurt, 60323 Frankfurt am Main, Germany.

^fAlso at Key Laboratory for Particle Physics, Astrophysics and Cosmology, Ministry of Education; Shanghai Key Laboratory for Particle Physics and Cosmology; Institute of Nuclear and Particle Physics, Shanghai 200240, People's Republic of China.

^gAlso at Key Laboratory of Nuclear Physics and Ion-beam Application (MOE) and Institute of Modern Physics, Fudan University, Shanghai 200443, People's Republic of China.

^hAlso at State Key Laboratory of Nuclear Physics and Technology, Peking University, Beijing 100871, People's Republic of China.

ⁱAlso at School of Physics and Electronics, Hunan University, Changsha 410082, China.

^jAlso at Guangdong Provincial Key Laboratory of Nuclear Science, Institute of Quantum Matter, South China Normal University, Guangzhou 510006, China.

^kAlso at MOE Frontiers Science Center for Rare Isotopes, Lanzhou University, Lanzhou 730000, People's Republic of China.

^lAlso at Lanzhou Center for Theoretical Physics, Lanzhou University, Lanzhou 730000, People's Republic of China.

^mAlso at the Department of Mathematical Sciences, IBA, Karachi 75270, Pakistan.

ⁿAlso at Ecole Polytechnique Federale de Lausanne (EPFL), CH-1015 Lausanne, Switzerland.

^oAlso at Helmholtz Institute Mainz, Staudinger Weg 18, D-55099 Mainz, Germany.

^pAlso at School of Physics, Beihang University, Beijing 100191, China.